

Article

Evaluation of Selected Properties of Dielectric Barrier Discharge Plasma Jet

Michał Kwiatkowski ¹, Piotr Terebun ¹, Katarína Kučerová ², Barbora Tarabová ³, Zuzana Kovalová ³, Aleksandra Lavrikova ², Zdenko Machala ², Karol Hensel ² and Joanna Pawłat ^{1,*}

¹ Chair of Electrical Engineering and Electrotechnologies, Lublin University of Technology, 20-618 Lublin, Poland

² Faculty of Mathematics, Physics and Informatics, Comenius University, 842 48 Bratislava, Slovakia

³ Institute of Plasma Physics of the Czech Academy of Sciences, Za Slovankou 3, 182 00 Prague, Czech Republic

* Correspondence: askmik@hotmail.com or j.pawlat@pollub.pl

Abstract: In the technological processes requiring mild treatment, such as soft materials processing or medical applications, an important role is played by non-equilibrium plasma reactors with dielectric barrier discharge (DBD), that when generated in noble gases allows for the effective treatment of biological material at a low temperature. The aim of this study is to determine the operating parameters of an atmospheric pressure, radio-frequency DBD plasma jet reactor for the precise treatment of biological materials. The tested parameters were the shape of the discharge (its length and volume), current and voltage signals, as well as the power consumed by the reactor for various composition and flow rates of the working gas. To determine the applicability in medicine, the temperature, pH, concentrations of H₂O₂, NO₂⁻ and NO₃⁻ and *Escherichia coli* log reduction in the plasma treated liquids were determined. The obtained results show that for certain operating parameters, a narrow shape of plasma stream can generate significant amounts of H₂O₂, allowing for the mild decontamination of bacteria at a relatively low power of the system, safe for the treatment of biological materials.

Keywords: atmospheric pressure plasma; dielectric barrier discharge; plasma jet; plasma treatment of liquid; reactive oxygen and nitrogen species; biological materials; *Escherichia coli*



Citation: Kwiatkowski, M.; Terebun, P.; Kučerová, K.; Tarabová, B.; Kovalová, Z.; Lavrikova, A.; Machala, Z.; Hensel, K.; Pawłat, J. Evaluation of Selected Properties of Dielectric Barrier Discharge Plasma Jet. *Materials* **2023**, *16*, 1167. <https://doi.org/10.3390/ma16031167>

Academic Editor: Daniela Caschera

Received: 14 December 2022

Revised: 23 January 2023

Accepted: 28 January 2023

Published: 30 January 2023



Copyright: © 2023 by the authors. Licensee MDPI, Basel, Switzerland. This article is an open access article distributed under the terms and conditions of the Creative Commons Attribution (CC BY) license (<https://creativecommons.org/licenses/by/4.0/>).

1. Introduction

Currently, one of the most important areas of the application of plasma technologies is the use of non-equilibrium plasma, where the energies of electrons are much higher than the energies of ions and neutral particles. The selectivity of energy and a low degree of ionization allow for chemical reactions initiated by high-energy electrons at a relatively low temperature of the working gas. In low-temperature plasma applications, systems with dielectric barrier discharge (DBD) are particularly popular, allowing to obtain a stable discharge without the presence of electric arcs. In the case of the treatment of biological and other heat-sensitive materials of various shapes, where it is necessary to limit the impact area and operate in ambient air, atmospheric pressure plasma jet (APPJ) systems are broadly used [1–6]. In these systems, the plasma generated inside the nozzle is blown towards the treated objects as a result of the forced gas flow. Particular systems of APPJ may differ in terms of the type of power supply, the discharge geometry and the composition of working gas. Due to the presence of a dielectric barrier, the reactors are powered by AC (including radio and microwave frequencies) or impulse voltage ranging from several to a dozen kilovolts. To obtain the lowest possible gas temperature while sustaining stable discharge, mixtures with the majority of noble gas (helium, argon) are used, and the power of the system rarely exceeds a dozen watts. Indirect treatment is often used in order to lower the temperature even further, in which the treated biological material is not in direct

contact with the plasma, but rather with active particles carried along with the gas stream (afterglow effect).

In medicine, DBD APPJ reactors have been used for the deactivation of pathogens [5,7–14], wound healing [9,14–16], stomatology [14,17,18] and anti-tumor treatment [14,19–21]. Examples of other low-temperature applications include surface modification [3,22–24] or improving agricultural seed germination [25–27]. Several effects of plasma treatment, such as UV-radiation and electric fields, are employed in the treatment of biological materials, but the most important of these remains the effect of reactive oxygen and nitrogen species (RONS) [28–30]. Plasma operating in atmospheric air in contact with liquids can generate significant amounts of various RONS in both gas and liquids phases, which are relevant for biological and environmental applications.

Advanced oxidation processes employ several kinds of environmentally friendly oxidants in the technological process allowing for superposition effect. Thus, they are considered the most efficient way of the removal of impurities, bactericidal decontamination and activation of surface. Electrical discharge can be generated directly in the treated liquid or in the gas intrusions in the liquid phase. Moreover, plasma can interact with the liquid indirectly when the discharge occurs in gaseous phase in the vicinity of the liquid surface and then active plasma species are further transferred via the surface to the bulk of the liquid [31–53].

When the discharge occurs in a multiphase environment, the nature of activated species strongly depends on actual composition of the liquid and the gas. Chemical processes that take place in the electrical discharges in water include direct formation of reactive radicals such as hydroxyl ($\bullet\text{OH}$), hydrogen (H), superoxide ($\text{O}_2\bullet^-$), perhydroxyl ($\text{HO}_2\bullet$) and oxide anions, and molecular species such as hydrogen peroxide (H_2O_2) and ozone (O_3). Nitrogen-based species are also produced, such as nitrogen oxide radicals ($\text{NO}\bullet$, $\text{NO}_2\bullet$), nitrate (NO_3^-) and nitrite (NO_2^-) anions, peroxyxynitrite (ONOO^-), and also nitric (HNO_3), nitrous (HNO_2) and peroxyxynitrous acids (ONOOH) (Table 1).

Table 1. Properties of selected oxygen base species [39,54–56].

Species	Formula	Standard Electrochemical Potential [V]	pH Where Present	Role
Hydroxyl radical	$\bullet\text{OH}$	+2.59	pH < 11.9	strong oxidant
Hydrogen peroxide	H_2O_2	+1.77	pH < 11.6	strong oxidant, weak reductant
Superoxide anion	$\text{O}_2\bullet^-$	−0.33	pH > 4.8	weak reductant
Perhydroxyl radical	$\text{HO}_2\bullet$	+1.49	pH < 4.8	strong oxidant
Hydroperoxide anion	HO_2^-	0.88	pH > 11.6	weak oxidant, weak reductant
Singlet oxygen	$^1\text{O}_2$			
Ozone gas	O_3	+2.07		strong oxidant
Atmospheric oxygen	O_2	+1.23		weak oxidant
Solvated electrons	$e_{(\text{aq})}^-$	−2.77	pH > 7.85	strong reductant
Nitrate anion	NO_3^-			oxidant in acidic solutions
Nitrite anion	NO_2^-			oxidant in reductant

Table 1. Cont.

Species	Formula	Standard Electrochemical Potential [V]	pH Where Present	Role
Peroxynitrite	ONOO ⁻			strong oxidant
Nitric oxide radical	NO•			reductant oxidant
Nitrogen dioxide radical	NO ₂ •			Oxidizing agent reducing agent

The group of Brisset et al. [39,52,57–59] investigated humid air plasmas and electrical discharges generated in contact with the surface of liquids. In such an environment, RONS derive from N₂, O₂ and H₂O, therefore hydrogen peroxide H₂O₂, ozone O₃, or nitrogen oxides NO_x are expected to form, although O₃ is not favored by the presence of water. Emission spectroscopy measurements of plasma in humid air revealed that •OH and NO• radicals are simultaneously present in the discharge, with a much higher density for strongly oxidizing •OH radicals than for NO• radicals. The later ones are known as parent molecules for acid derivatives HNO₂ and HNO₃, inducing a rapid pH lowering of the solution. Thus, the presence of both •OH and NO• radicals can enhance the efficacy of the treatment process [57,60–65].

Plasma formed species are mainly considered with plasma–liquid interactions and induce acidification and oxidation reactions. The acidification effect is related to the formation of transient nitrous acid HNO₂ (which disproportionates into NO and nitric acid for pH < 6) and stable nitric acid HNO₃. A weak peroxyntrous acid ONOOH (pKa = 6.8) is also formed under certain conditions. The oxidizing character of plasma treatments is mainly attributed to •OH, H₂O₂ and ONOOH. Apart from these basic reactions, peroxyntrous acid ONOOH and its matching ion, peroxyntrite ONOO⁻, react as nitrosating and nitrating agents on double bonds and carboxylic acids. That makes them the key agents for bacterial inactivation because of their chemical attack at the microorganism membranes [39,59,66].

The aim of this study is to determine the optimal operating parameters and the possibility of generating active plasma species for plasma medical applications in helium DBD APPJ powered by radio frequency power supply. The tested parameters are discharge shape (its length and volume), electrical signals for different composition and flow rates of the working gas. To investigate the possibility of using the reactor in medicine, the temperature and concentrations of selected RONS (H₂O₂, NO₂⁻, NO₃⁻) in non-buffered and buffered liquids are examined, as well as the effect of the plasma treatment on the reduction of *E. coli* bacteria in these liquids.

2. Materials and Methods

The tested reactor was the DBD APPJ reactor in a system with two ring-shaped electrodes wrapped around a ceramic tube of 1.5/2.5 mm inner/outer diameter. Plasma was generated inside a tube and then directed towards the treated object by the forced gas flow, as shown in Figure 1.

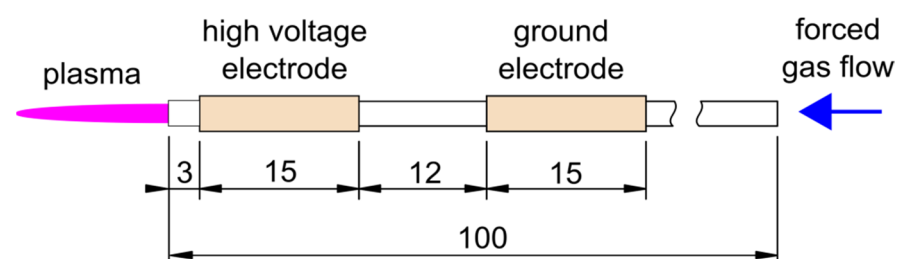


Figure 1. Geometry of DBD APPJ reactor, dimensions are given in mm.

The reactor was powered by a 20 kHz high-voltage power supply using a fly-back transformer. The voltage between electrodes U_2 was measured with a high-voltage probe (Tektronix P6015A, Berkshire, UK) connected to a digital oscilloscope (Tektronix TBS 2102, Berkshire, UK). The total current I_2 was measured indirectly by measuring the voltage (Tektronix P2220, Berkshire, UK) across a 100 Ohm low-inductive resistor (ARCOL AP101 R100, Munich, Germany), as shown in Figure 2. In order to compare the efficiency of the system for various conditions, the power P_1 and S_1 at the input of the power supply was also measured with a wattmeter (Wattman, HPM-100A, AD POWER Co., Ltd., Bucheon-si, Republic of Korea).

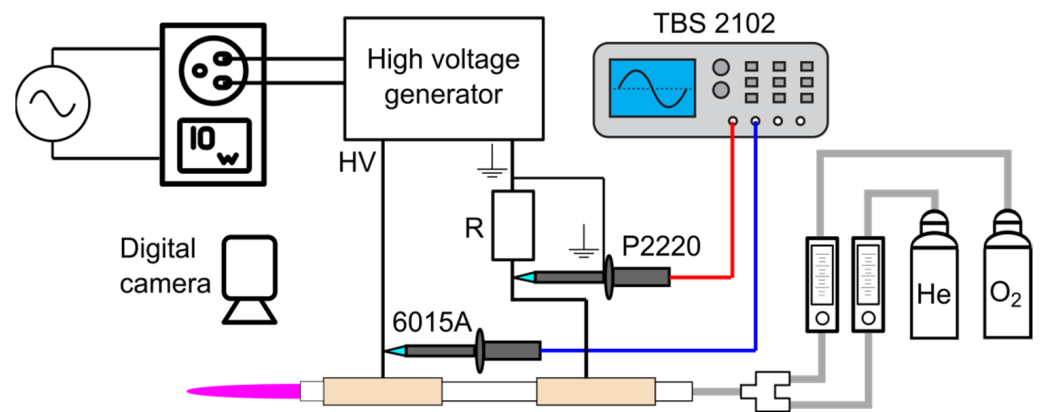


Figure 2. Experimental setup for measuring electrical quantities.

Helium and its mixture with oxygen were used for all experiments. During the tests, gases were fed through glass tube flow meters (Brooks Instrument SHO-RATE, Hatfield, PA, USA). The widest range of flow rates (0.32–5.8 L/min) was used in the study of the influence of the working gas on the shape of the discharge, which was carried out on the basis of the length of the glowing part of the plasma depicted on photos (Nikon D7000, Bratislava, Slovakia; 1/80 s exposure time) and known dimensions of reference points.

A study on the efficiency of generating selected compounds in aqueous phase and the decontamination effect on *Escherichia coli* was performed for two liquids: simulated tap “water” (NaH₂PO₄ solution, pH ~ 5, σ ~ 600 μ S/cm) and 2 mM “PB” (phosphate buffer solution, pH ~ 7, σ ~ 560 μ S/cm). The concentrations of selected species (H₂O₂, NO₂[−], NO₃[−]) were determined by the colorimetric method described in our previous publication [67], using reagents and absorbance wavelength presented in Table 2. For the verification of the results, the standard error of the mean from two repetitions were used.

Table 2. Conditions for colorimetric method.

Compound	Reagents	Maximum Absorption
H ₂ O ₂	TiOSO ₄ solution	407 nm
NO ₂ [−]	Griess assay	540 nm
NO ₃ [−]	Enzymatic reduction to NO ₂ [−] + Griess assay	540 nm

During the measurements, 2 mL of the liquid was placed in a 24-well plate at 15 mm distance between the nozzle and the treated liquid sample (Figure 3). Measurements were performed for 2 and 5 min of plasma treatment. The reference (control) samples were tested for 5 min action of the gas directed to the surface of the liquid. The temperature of the liquid was measured immediately after plasma treatment using an uninsulated K-type thermocouple with an electronic temperature compensation meter (Yu Ching Technology DT-847U), noting the highest meter reading within 10 s.

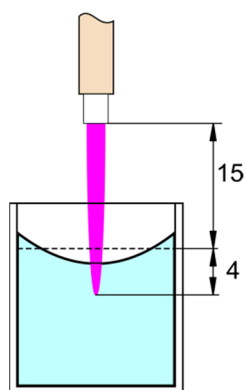


Figure 3. Experimental setup for chemical and biological treatment. The plasma jet impinges on the liquid surface and slightly dives into the liquid.

For the same distance, biological treatment was performed for planktonic *E. coli* (CCM3945) dissolved from gel disc in “water” or “PB”. A pellet of *E. coli* was suspended in 10 mL of desired aqueous solution and let at 35 °C for 18 h, then 5 ml of this suspension was added to 45 ml of “water” or “PB” solution. The obtained initial concentration of bacteria was $\sim 10^6$ – 10^7 CFU/mL (colony forming unit per milliliter). After plasma treatment, the sample was diluted and cultivated on agar plates overnight. The control samples were processed the same way except the (discharge) plasma was not applied. Then colonies were counted and logarithmic reduction was evaluated as a difference of CFU for controls and samples. For statistical interpretations, median and interquartile range from 4 repetitions were used.

In addition, measurements of pH were performed by pH-meter.

3. Results

3.1. Discharge Images

Examples of the discharge images for different gas flow rates are shown in Figure 4. A comparison of the obtained results shows a very strong influence of the flow rate value on the discharge shape, which becomes turbulent for too high flow rates (>3.5 L/min). The highest discharge volume was obtained at a flow rate of 1.5 L/min and this value was chosen as the reference for the following studies. The addition of oxygen admixture to He resulted in a reduction in the length and volume of the discharge, therefore an oxygen addition of 0.3 L/min was selected for further measurements, for which a similar discharge length was still obtained.

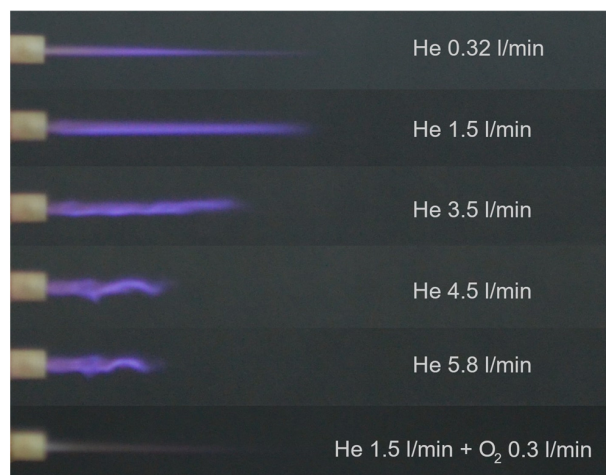


Figure 4. The shape of the discharge for different gas flow rates and composition of the mixture.

3.2. Electrical Characteristics

The waveforms of the voltage U_2 signal and the current I_2 drawn from the high-voltage power supply are shown in Figures 5 and 6.

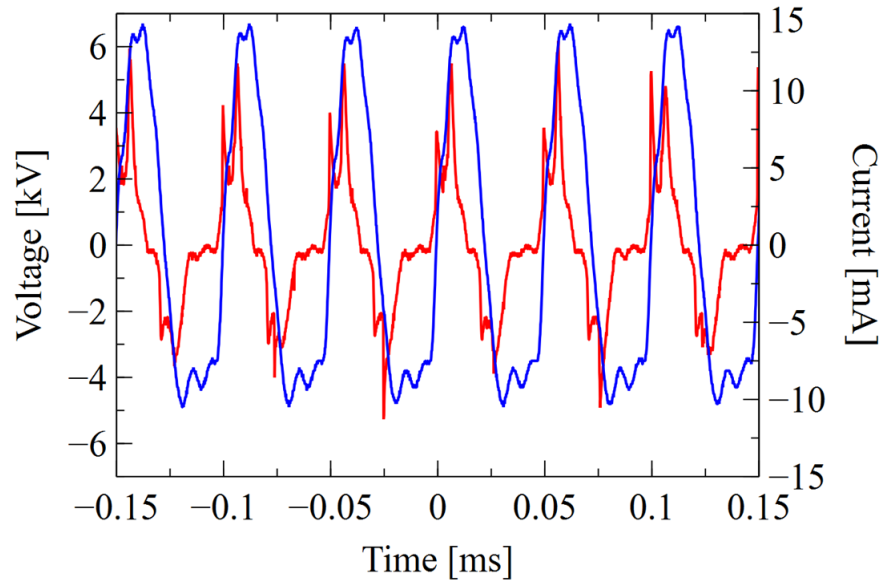


Figure 5. Waveform of voltage (blue line) and current (red line) for 1.5 L/min helium.

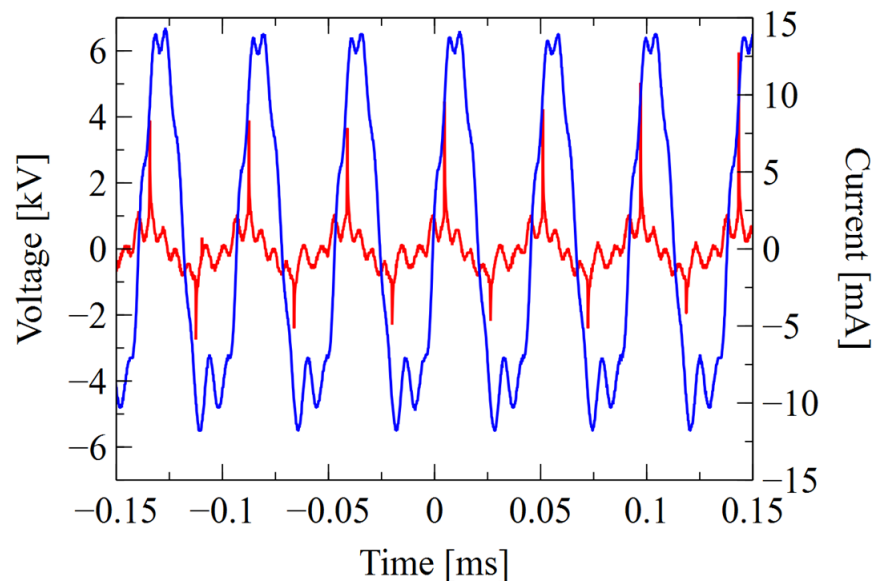


Figure 6. Waveform of voltage (blue line) and current (red line) for 1.5 L/min helium and 0.3 L/min oxygen mixture.

The measurement results and the calculated active (P) and apparent (S) power values are summarized in Table 3. Active power (P) refers to the part of power that is absorbed by the load (plasma) and usually is smaller than the apparent power (S) that is a product of voltage and current. For both gas compositions, the system is capacitive. In the case of mixture of helium and oxygen ($\text{He}+\text{O}_2$), despite similar voltages, the total current in the system is several times lower, which is also reflected in the power consumed by the supply system. For this system, based on the power ratio, a significant decrease in the efficiency of the power supply can also be noticed.

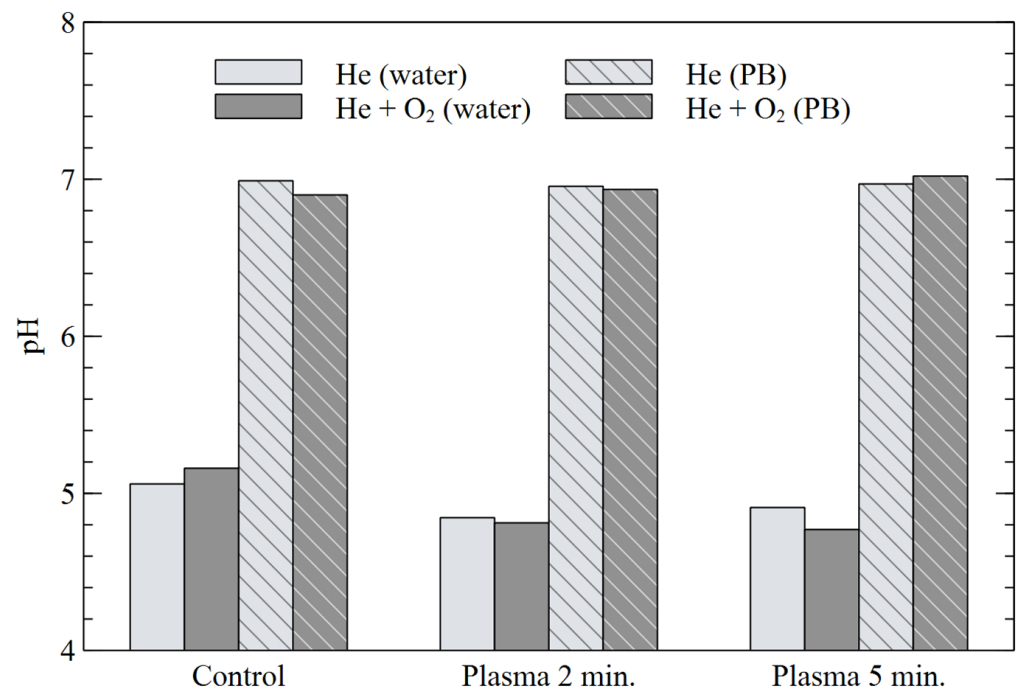
Table 3. Electrical parameters of the reactor for used gas mixtures.

Mixture	P_1 [W]	$U_{2\text{RMS}}$ [kV]	$I_{2\text{RMS}}$ [mA]	P_2 [W]	S_2 [VA]
He	11.09	4.15	4.25	10.24	17.67
He+O ₂	4.6	4.17	1.38	2.96	5.76

3.3. Chemical and Biological Analysis

Prior to plasma treatment, the liquids were kept at room temperature (20 °C). For all tested conditions, the liquid temperature after plasma treatment did not exceed 25 °C.

Figure 7 shows pH values of the liquids after the 2 and 5 min treatments. Plasma treatment resulted in a slight decrease of pH value of “water”, which is more noticeable with a mixture of He+O₂. For the “PB” solution, no significant difference in pH was observed even after 5 min of treatment. These values are consistent with our formerly-obtained results [7,38,39,52]. Gaseous nitrogen oxides NO_x were generated in plasma jet surrounded by ambient air and further transported to the liquid phase, where nitrate NO₃[−] and nitrite NO₂[−] anions accompanied with hydronium ions H₃O⁺ were formed. Consequently, reaction of NO₂[−] with H₃O⁺ ions resulted in an acidic product: nitrous acid HNO₂, which caused a slight pH decrease of “water”. The aim of the phosphate buffer (PB) solution was to investigate the pH impact on the other parameters of plasma-treated liquids. Presented results confirm that phosphate buffer was not affected by plasma.

**Figure 7.** Measurements of pH of water and PB for different plasma treatment times.

The results of the H₂O₂ concentration in the solutions are shown in Figure 8. For both treatment times, a much higher concentration was observed for He alone than for its He+O₂ mixture, although the results for the second mixture were more reproducible. The presence of the buffer did not significantly affect the results, except for the “water” 5-min treatment with He alone, for which the highest concentration was obtained. The relationship between H₂O₂ concentration and treatment time is almost linear, however, for NO_x[−] compounds, the chemistry of the chemical reactions is not so simple. Figure 9 shows the results obtained for the NO₂[−] concentration. Much significant and more reproducible changes were observed in He alone. In this case, slightly higher concentrations are also seen for the “PB” solution. Increasing the treatment time from 2 to 5 min resulted in a slight

increase in the concentrations in He, and over triple increase in the NO₂⁻ concentration for the mixture of He+O₂.

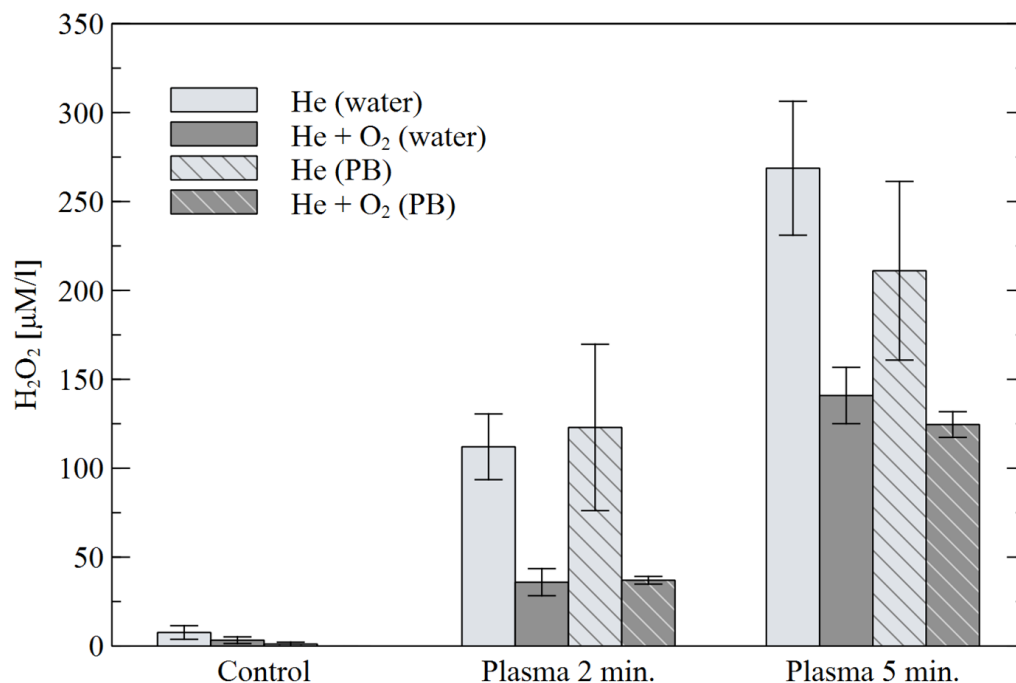


Figure 8. Concentration of H₂O₂ in water and PB for different plasma treatment times.

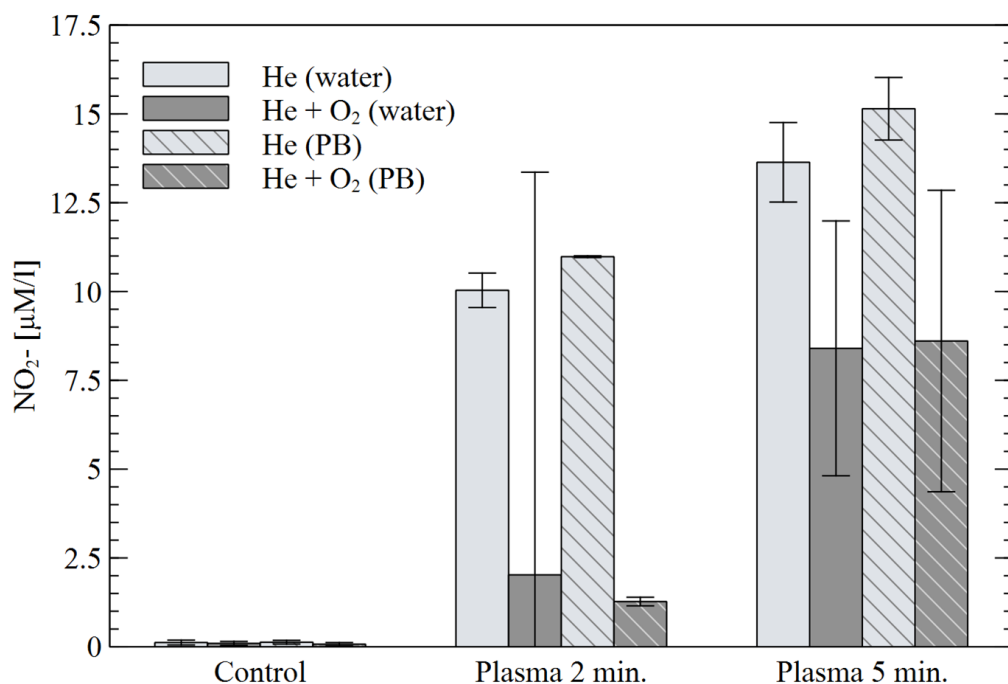


Figure 9. Concentration of NO₂⁻ in water and PB for different plasma treatment times.

The concentration of nitrates NO₃⁻ for the 2- and 5-min plasma treatments is shown in Figure 10. For both working gases, the concentration of NO₃⁻ is higher for the “PB” liquid, while for the mixture of He+O₂ the difference is more than double. In this case, the addition of oxygen caused a much greater amount of NO₃⁻ compared to He alone.

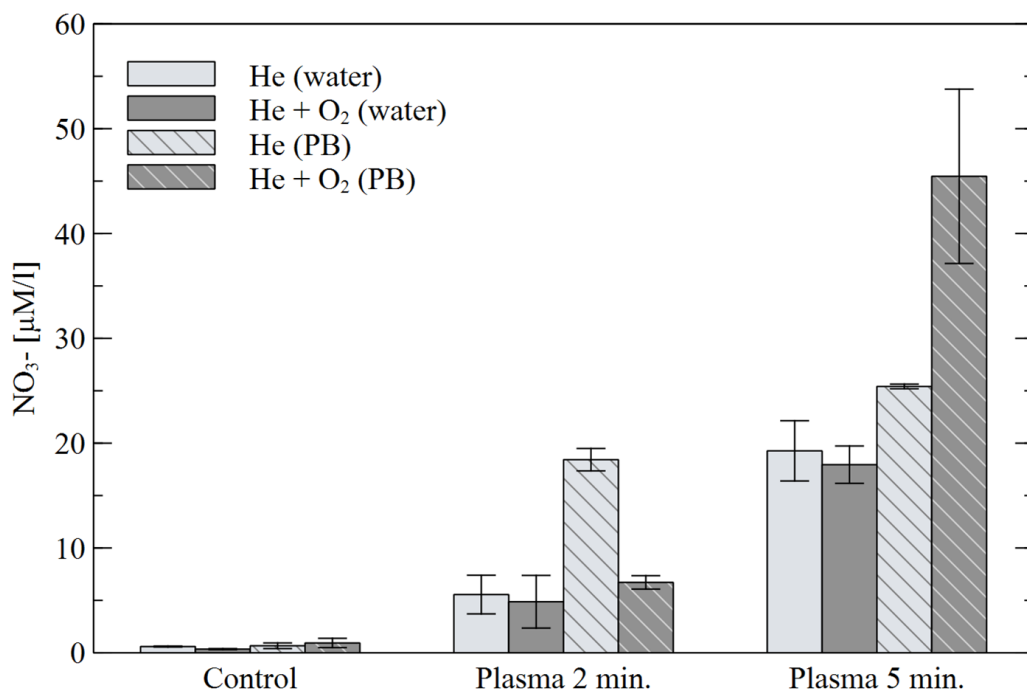


Figure 10. Concentration of NO₃⁻ in water and PB for different treatment times.

Figure 11 shows the effect of plasma treatment on the reduction of *E. coli* suspended in water or PB. Better antibacterial results were obtained for the mixture of He+O₂. However, the observed bacterial reduction for both mixtures is significant but relatively small. For both gases, the use of the “PB” solution significantly lowered the treatment efficiency.

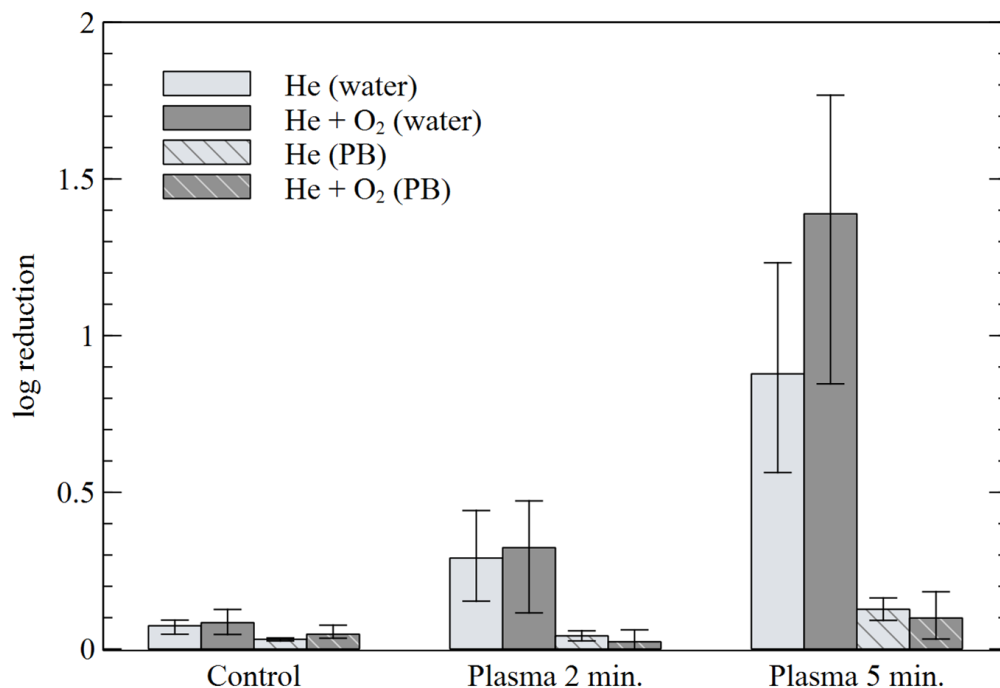


Figure 11. Logarithmic reduction of *E. coli* in aqueous water and PB solutions for different treatment times.

4. Discussion and Conclusions

The DBD APPJ discharge images show a strong influence of the working gas on the shape (length, volume) of the generated plasma. The most important factor influenc-

ing the shape of the plasma jet is the gas flow rate, which is also often observed in the literature [2,68–71]. A small addition of oxygen, introduced to increase the amount of RONS, decreased the length of the glowing part of the discharge. It may be related to a lower degree of ionization for non-noble gas admixture, however the reduction of the amount and mobility of charges and a visible decrease of the discharge current did not significantly change the shape of the discharge itself, which had a narrow shape suitable for focalized point treatment of biological objects.

When analyzing the measured voltage and current signals, apart from the phase shift related to the capacitive nature of the load, a certain asymmetry of the half-periods of signals can be observed. The current peaks associated with micro-discharges, due to the large differences between individual gas mixtures, have a higher magnitude and less phase shift for the positive part of signal than for the negative part, which is well visible in He working gas. The time intervals between the current and voltage peaks also differ, which indicates the influence of the accumulated charge on the dielectric surface. Uneven charging may be related to the geometry of the system and plasma propagation in the direction of the gas flow. It can cause both a different value and number of micro-discharges in particular cycles [72–74]. In the case of the used power supply, the discharge current peaks also influence the shape of the voltage between the electrodes, which dropped significantly in time intervals corresponding to micro-discharges.

Much lower values of the peak current obtained for the oxygen-containing mixture were also reflected in the power and efficiency of the system. For a mixture of He+O₂, the active and apparent power drawn from the source is much lower than that for He alone, but utilization of the active power part used by the load is much lower. It is related to the lower value of the micro-discharge current with the same value of the displacement current, which reduces the overall efficiency of the entire system.

Due to the low discharge currents, the power of the system for both tested gas mixtures was relatively low. This is reflected in the temperature of the treated liquid, which only slightly increased after the 5 min treatment. Despite the low power, the reactor allows for the generation of H₂O₂, NO₂[−] and NO₃[−] and their transport to the liquid phase. In the case of hydrogen peroxide H₂O₂, the relationship between the concentration and the treatment time is almost linear. In terms of the amount of generated H₂O₂, this DBD APPJ system is more energy-efficient than the mini-gliding arc reactor tested in the past with the same diagnostic methods [67]. This may be related to the better transport of the active species along with the plasma stream which is in contact with the liquid and the possibility of generating H₂O₂ directly in it.

On the other hand, the amount of generated NO_x compounds is relatively small, which is also consistent with only a slight pH drop. Despite the possibility of interaction with nitrogen N₂ present in the atmospheric air surrounding the discharge [75], plasma occurs mainly in the working gas, the components of which are transferred along with the stream to the liquid but the energy delivery is much weaker here than in more powerful plasma discharges, e.g., mini-gliding arc or transient spark [7,67]. Due to the small concentrations of nitrogen compounds and the more complex chemistry involved in both the liquid reactions and the reagents used to determine their concentrations, the results are not as well reproducible as for H₂O₂. The obtained low concentrations, however, may have contributed to the high H₂O₂ content, through preventing the decomposition of H₂O₂ by its reaction with NO₂[−] [76].

The obtained RONS concentrations also allowed the reduction of *E. coli*, which may be related to the decontamination effect of H₂O₂ [30,77]. However, the pH-dependence of the effect even for a slight pH drop to 4.8 in water most likely indicates an additional role of ONOOH formation in bacterial reduction, via the reaction of H₂O₂ and low concentration of NO₂[−]. The log reduction of bacteria here is lower than other DBD APPJ reactors [78,79] but similar to the results obtained in the liquid phase [77]. Due to the low power of the reactor and the narrow shape of plasma stream, these results seem to be sufficient for the practical application of tested DBD-APPJ in medicine where microorganisms need

to be selectively inactivated without harming the healthy tissue cells. Examples include precise biomedical treatments, such as wound healing, oral cavity infections or focalized tumor treatments. An additional advantage of the presented low-power DBD APPJ is also the indirect nature of the treatment, where the discharge taking place mainly between the electrodes of the reactor and the target is mildly treated by its reactive effluent, thus preventing the complexity and danger of applying high voltage directly to the biological targets, where a similar plasma jet reactors are the subject of worldwide research [30].

Author Contributions: Conceptualization, J.P., Z.M. and K.H.; methodology, M.K., J.P. and K.H.; validation, J.P. and K.H.; formal analysis, M.K., P.T., K.K., B.T., Z.K. and A.L.; investigation, M.K., P.T., K.K., B.T., Z.K. and A.L.; data curation, P.T. and K.H.; writing—original draft preparation, P.T. and M.K.; writing—review and editing, J.P. and K.H.; visualization, P.T.; supervision, Z.M., K.H. and J.P.; funding acquisition, K.H., Z.M. and J.P. All authors have read and agreed to the published version of the manuscript.

Funding: This publication was founded in the framework of the activities of the Polish Metrological Union are financed from the funds of the Ministry of Education and Science as part of a targeted subsidy for the implementation of the task titled "Establishment and Coordination of the activities of the Polish Metrological Union (PMU)" under contract no. MEiN/2021/DPI/179. Research was supported by; Slovak Research and Development Agency Grants: APVV-17-0382 and APVV-20-0566, Project No. 2016/22/Z/ST8/00694; Slovak Grant Agency VEGA grants 1/0822/21 and 1/0596/22.

Institutional Review Board Statement: Not applicable.

Informed Consent Statement: Not applicable.

Data Availability Statement: Data available upon justified request after contact with authors.

Acknowledgments: We are grateful the fruitful discussions in the following cooperative initiatives: COST Actions CA19110 (Plasma applications for smart and sustainable agriculture), CA20114 (Therapeutical applications of Cold Plasmas); CEEPUS CIII-AT-0063, Inkubator Innowacyjności Politechnika Lubelska, and Polish-Slovak Bilateral Cooperation Programme (PlasmaBioAgro) PPN/BIL/2018/1/00065.

Conflicts of Interest: The authors declare no conflict of interest.

References

1. Laroussi, M.; Akan, T. Arc-Free Atmospheric Pressure Cold Plasma Jets: A Review. *Plasma Process. Polym.* **2007**, *4*, 777–788. [\[CrossRef\]](#)
2. Fanelli, F.; Fracassi, F. Atmospheric Pressure Non-Equilibrium Plasma Jet Technology: General Features, Specificities and Applications in Surface Processing of Materials. *Surf. Coat. Technol.* **2017**, *322*, 174–201. [\[CrossRef\]](#)
3. Penkov, O.; Khadem, M.; Lim, W.-S.; Kim, D.-E. A Review of Recent Applications of Atmospheric Pressure Plasma Jets for Materials Processing. *J. Coat. Technol. Res.* **2015**, *12*, 225–235. [\[CrossRef\]](#)
4. Lu, X.; Laroussi, M.; Puech, V. On Atmospheric-Pressure Non-Equilibrium Plasma Jets and Plasma Bullets. *Plasma Sources Sci. Technol.* **2012**, *21*, 034005. [\[CrossRef\]](#)
5. Weltmann, K.D.; Kindel, E.; von Woedtke, T.; Hähnel, M.; Stieber, M.; Brandenburg, R. Atmospheric-Pressure Plasma Sources: Prospective Tools for Plasma Medicine. *Pure Appl. Chem.* **2010**, *82*, 1223–1237. [\[CrossRef\]](#)
6. Laroussi, M. Low Temperature Plasma Jets: Characterization and Biomedical Applications. *Plasma* **2020**, *3*, 54–58. [\[CrossRef\]](#)
7. Hensel, K.; Kučerová, K.; Tarabová, B.; Janda, M.; Machala, Z.; Sano, K.; Mihai, C.T.; Ciorpac, M.; Gorgan, L.D.; Jijie, R.; et al. Effects of Air Transient Spark Discharge and Helium Plasma Jet on Water, Bacteria, Cells, and Biomolecules. *Biointerphases* **2015**, *10*, 029515. [\[CrossRef\]](#)
8. Daeschlein, G.; Scholz, S.; von Woedtke, T.; Niggemeier, M.; Kindel, E.; Brandenburg, R.; Weltmann, K.; Jünger, M. In Vitro Killing of Clinical Fungal Strains by Low-Temperature Atmospheric-Pressure Plasma Jet. *IEEE Trans. Plasma Sci.* **2011**, *39*, 815–821. [\[CrossRef\]](#)
9. Daeschlein, G.; Napp, M.; von Podewils, S.; Lutze, S.; Emmert, S.; Lange, A.; Klare, I.; Haase, H.; Gümbel, D.; von Woedtke, T.; et al. In Vitro Susceptibility of Multidrug Resistant Skin and Wound Pathogens Against Low Temperature Atmospheric Pressure Plasma Jet (APPJ) and Dielectric Barrier Discharge Plasma (DBD). *Plasma Process. Polym.* **2014**, *11*, 175–183. [\[CrossRef\]](#)
10. Guimin, X.; Guanjun, Z.; Xingmin, S.; Yue, M.; Ning, W.; Yuan, L. Bacteria Inactivation Using DBD Plasma Jet in Atmospheric Pressure Argon. *Plasma Sci. Technol.* **2009**, *11*, 83–88. [\[CrossRef\]](#)

11. Svarnas, P.; Spiliopoulou, A.; Koutsoukos, P.G.; Gazeli, K.; Anastassiou, E.D. Acinetobacter Baumannii Deactivation by Means of DBD-Based Helium Plasma Jet. *Plasma* **2019**, *2*, 77–90. [[CrossRef](#)]
12. Mazánková, V.; Sťahel, P.; Matoušková, P.; Brablec, A.; Čech, J.; Prokeš, L.; Buršíková, V.; Stupavská, M.; Lehocký, M.; Ozaltın, K.; et al. Atmospheric Pressure Plasma Polymerized 2-Ethyl-2-Oxazoline Based Thin Films for Biomedical Purposes. *Polymers* **2020**, *12*, 2679. [[CrossRef](#)] [[PubMed](#)]
13. Jirásek, V.; Koval'ová, Z.; Tarabová, B.; Lukeš, P. Leucine Modifications by He/O₂ Plasma Treatment in Phosphate-Buffered Saline: Bactericidal Effects and Chemical Characterization. *J. Phys. D Appl. Phys.* **2021**, *54*, 505206. [[CrossRef](#)]
14. Laroussi, M.; Bekeschus, S.; Keidar, M.; Bogaerts, A.; Fridman, A.; Lu, X.; Ostrikov, K.; Hori, M.; Stapelmann, K.; Miller, V.; et al. Low-Temperature Plasma for Biology, Hygiene, and Medicine: Perspective and Roadmap. *IEEE Trans. Radiat. Plasma Med. Sci.* **2022**, *6*, 127–157. [[CrossRef](#)]
15. Shahbazi Rad, Z.; Abbasi Davani, F. Measurements of the Electrical Parameters and Wound Area for Investigation on the Effect of Different Non-Thermal Atmospheric Pressure Plasma Sources on Wound Healing Time. *Measurement* **2020**, *155*, 107545. [[CrossRef](#)]
16. Heinlin, J.; Morfill, G.; Landthaler, M.; Stolz, W.; Isbary, G.; Zimmermann, J.L.; Shimizu, T.; Karrer, S. Plasma Medicine: Possible Applications in Dermatology. *JDDG: J. Der Dtsch. Dermatol. Ges.* **2010**, *8*, 968–976. [[CrossRef](#)]
17. Yang, Y.; Zheng, M.; Yang, Y.; Li, J.; Su, Y.-F.; Li, H.-P.; Tan, J.-G. Inhibition of Bacterial Growth on Zirconia Abutment with a Helium Cold Atmospheric Plasma Jet Treatment. *Clin Oral Invest* **2020**, *24*, 1465–1477. [[CrossRef](#)] [[PubMed](#)]
18. Xiong, Z.; Cao, Y.; Lu, X.; Du, T. Plasmas in Tooth Root Canal. *IEEE Trans. Plasma Sci.* **2011**, *39*, 2968–2969. [[CrossRef](#)]
19. Tomić, S.; Petrović, A.; Puač, N.; Škoro, N.; Bekić, M.; Petrović, Z.L.; Čolić, M. Plasma-Activated Medium Potentiates the Immunogenicity of Tumor Cell Lysates for Dendritic Cell-Based Cancer Vaccines. *Cancers* **2021**, *13*, 1626. [[CrossRef](#)] [[PubMed](#)]
20. Vandamme, M.; Robert, E.; Pesnel, S.; Barbosa, E.; Dozias, S.; Sobilo, J.; Lerondel, S.; Pape, A.L.; Pouvesle, J.-M. Antitumor Effect of Plasma Treatment on U87 Glioma Xenografts: Preliminary Results. *Plasma Process. Polym.* **2010**, *7*, 264–273. [[CrossRef](#)]
21. Utsumi, F.; Kajiyama, H.; Nakamura, K.; Tanaka, H.; Mizuno, M.; Ishikawa, K.; Kondo, H.; Kano, H.; Hori, M.; Kikkawa, F. Effect of Indirect Nonequilibrium Atmospheric Pressure Plasma on Anti-Proliferative Activity against Chronic Chemo-Resistant Ovarian Cancer Cells In Vitro and In Vivo. *PLoS ONE* **2013**, *8*, e81576. [[CrossRef](#)] [[PubMed](#)]
22. Cheng, K.-Y.; Chang, C.-H.; Yang, Y.-W.; Liao, G.-C.; Liu, C.-T.; Wu, J.-S. Enhancement of Cell Growth on Honeycomb-Structured Polylactide Surface Using Atmospheric-Pressure Plasma Jet Modification. *Appl. Surf. Sci.* **2017**, *394*, 534–542. [[CrossRef](#)]
23. Cheng, C.; Liye, Z.; Zhan, R.-J. Surface Modification of Polymer Fibre by the New Atmospheric Pressure Cold Plasma Jet. *Surf. Coat. Technol.* **2006**, *200*, 6659–6665. [[CrossRef](#)]
24. Ma, C.; Nikiforov, A.; De Geyter, N.; Morent, R.; Ostrikov, K. (Ken) Plasma for Biomedical Decontamination: From Plasma-Engineered to Plasma-Active Antimicrobial Surfaces. *Curr. Opin. Chem. Eng.* **2022**, *36*, 100764. [[CrossRef](#)]
25. Bafoil, M.; Jemmat, A.; Martinez, Y.; Merbahi, N.; Eichwald, O.; Dunand, C.; Yousfi, M. Effects of Low Temperature Plasmas and Plasma Activated Waters on Arabidopsis Thaliana Germination and Growth. *PLoS ONE* **2018**, *13*, e0195512. [[CrossRef](#)] [[PubMed](#)]
26. Alves Junior, C.; de Oliveira Vitoriano, J.; da Silva, D.L.S.; de Lima Farias, M.; de Lima Dantas, N.B. Water Uptake Mechanism and Germination of Erythrina Velutina Seeds Treated with Atmospheric Plasma. *Sci. Rep.* **2016**, *6*, 33722. [[CrossRef](#)]
27. Pawlat, J.; Starek, A.; Sujak, A.; Terebun, P.; Kwiatkowski, M.; Budzeń, M.; Andrejko, D. Effects of Atmospheric Pressure Plasma Jet Operating with DBD on Lavatera Thuringiaca L. Seeds' Germination. *PLoS ONE* **2018**, *13*, e0194349. [[CrossRef](#)]
28. von Woedtke, T.; Reuter, S.; Masur, K.; Weltmann, K.-D. Plasmas for Medicine. *Phys. Rep.* **2013**, *530*, 291–320. [[CrossRef](#)]
29. Lu, X.; Naidis, G.V.; Laroussi, M.; Reuter, S.; Graves, D.B.; Ostrikov, K. Reactive Species in Non-Equilibrium Atmospheric-Pressure Plasmas: Generation, Transport, and Biological Effects. *Phys. Rep.* **2016**, *630*, 1–84. [[CrossRef](#)]
30. Reuter, S.; von Woedtke, T.; Weltmann, K.-D. The KINPen—A Review on Physics and Chemistry of the Atmospheric Pressure Plasma Jet and Its Applications. *J. Phys. D Appl. Phys.* **2018**, *51*, 233001. [[CrossRef](#)]
31. Pawlat, J.; Yamabe, C.; Pollo, I. Generation of Discharges in Dynamic Foam for Oxidants Formation Using Various Types of Electrodes. *Colloids Surf. A Physicochem. Eng. Asp.* **2003**, *220*, 179–190. [[CrossRef](#)]
32. De Laat, J.; Berger, P.; Poinot, T.; vel Leitner, N.K.; Doré, M. Modeling the Oxidation of Atrazine by H₂O₂/UV. Estimation of Kinetic Parameters. *Ozone Sci. Eng.* **1997**, *19*, 395–408. [[CrossRef](#)]
33. Gehringer, P.; Szinovatz, W.; Eschweiler, H.; Haberl, R. Oxidative Treatment of a Wastewater Stream from a Molasses Processing Using Ozone and Advanced Oxidation Technologies. *Ozone Sci. Eng.* **1997**, *19*, 157–168. [[CrossRef](#)]
34. Pawlat, J.; Hayashi, N.; Ihara, S.; Satoh, S.; Yamabe, C.; Pollo, I. Foaming Column with a Dielectric Covered Plate-to-Metal Plate Electrode as an Oxidants' Generator. *Adv. Environ. Res.* **2004**, *8*, 351–358. [[CrossRef](#)]
35. Karimi, A.A.; Redman, J.A.; Stolarik, G.F.; Glaze, W.H. Evaluating an Aop for Tce and Pce Removal. *J. Am. Water Work. Assoc.* **1997**, *89*, 41–53. [[CrossRef](#)]
36. Sentek, J.; Krawczyk, K.; Młotek, M.; Kalczewska, M.; Kroker, T.; Kolb, T.; Schenk, A.; Gericke, K.-H.; Schmidt-Szałowski, K. Plasma-Catalytic Methane Conversion with Carbon Dioxide in Dielectric Barrier Discharges. *Appl. Catal. B Environ.* **2010**, *94*, 19–26. [[CrossRef](#)]
37. Pawlat, J.; Hensel, K.; Ihara, S. Decomposition of Humic Acid and Methylene Blue by Electric Discharge in Foam. *Acta Phys. Slovaca* **2005**, *55*, 479–485.

38. Bruggeman, P.J.; Kushner, M.J.; Locke, B.R.; Gardeniers, J.G.; Graham, W.G.; Graves, D.B.; Hofman-Caris, R.C.H.M.; Maric, D.; Reid, J.P.; Ceriani, E.; et al. Plasma–Liquid Interactions: A Review and Roadmap. *Plasma Sources Sci. Technol.* **2016**, *25*, 053002. [[CrossRef](#)]
39. Pawlat, J. *Electrical Discharges in Humid Environments. Generators, Effects, Application*; Monografie—Politechnika Lubelska; Politechnika Lubelska: Lublin, Poland, 2013; ISBN 978-83-63569-37-2.
40. Dors, M.; Metel, E.; Mizeraczyk, J. Phenol Degradation in Water by Pulsed Streamer Corona Discharge and Fenton Reaction. *Int. J. Plasma Environ. Sci. Technol.* **2007**, *1*, 76–81.
41. Dors, M.; Mizeraczyk, J.; Mok, Y.S. Phenol Oxidation in Aqueous Solution by Gas Phase Corona Discharge. *J. Adv. Oxid. Technol.* **2006**, *9*, 139–143. [[CrossRef](#)]
42. Srinivasan, B.; Palanki, S.; Grymonpré, D.R.; Locke, B.R. Optimization of a Continuous Pulsed Corona Reactor. *Chem. Eng. Sci.* **2001**, *56*, 1035–1039. [[CrossRef](#)]
43. Locke, B.R.; Sato, M.; Sunka, P.; Hoffmann, M.R.; Chang, J.-S. Electrohydraulic Discharge and Nonthermal Plasma for Water Treatment. *Ind. Eng. Chem. Res.* **2006**, *45*, 882–905. [[CrossRef](#)]
44. Lukes, P.; Appleton, A.T.; Locke, B.R. Hydrogen Peroxide and Ozone Formation in Hybrid Gas-Liquid Electrical Discharge Reactors. *IEEE Trans. Ind. Appl.* **2004**, *40*, 60–67. [[CrossRef](#)]
45. Lukes, P.; Clupek, M.; Babicky, V.; Sunka, P.; Winterova, G.; Janda, V. Non-Thermal Plasma Induced Decomposition of 2-Chlorophenol in Water. *Acta Phys. Slovaca* **2003**, *53*, 423–428.
46. Lukes, P.; Clupek, M.; Sunka, P.; Peterka, F.; Sano, T.; Negishi, N.; Matsuzawa, S.; Takeuchi, K. Degradation of Phenol by Underwater Pulsed Corona Discharge in Combination with TiO₂ Photocatalysis. *Res. Chem. Intermed.* **2005**, *31*, 285–294. [[CrossRef](#)]
47. Lukes, P.; Locke, B.R. Degradation of Substituted Phenols in a Hybrid Gas–Liquid Electrical Discharge Reactor. *Ind. Eng. Chem. Res.* **2005**, *44*, 2921–2930. [[CrossRef](#)]
48. Lukeš, P. *Water Treatment by Pulsed Streamer Corona Discharge*; Institute of Plasma Physics, AS CR: Prague, Czech Republic, 2001.
49. Stará, Z.; Krčma, F.; Nejezchleb, M.; Dušan Skalný, J. Organic Dye Decomposition by DC Diaphragm Discharge in Water: Effect of Solution Properties on Dye Removal. *Desalination* **2009**, *239*, 283–294. [[CrossRef](#)]
50. Schmidt-Szałowski, K.; Krawczyk, K.; Sentek, J.; Ulejczyk, B.; Górska, A.; Młotek, M. Hybrid Plasma-Catalytic Systems for Converting Substances of High Stability, Greenhouse Gases and VOC. *Chem. Eng. Res. Des.* **2011**, *89*, 2643–2651. [[CrossRef](#)]
51. Tuhkanen, T.A.; Kainulainen, T.K.; Vartiainen, T.K.; Kalliokoski, P.J. The Effect Of Preozonation, Ozone/Hydrogen Peroxide Treatment, And Nanofiltration On The Removal Of Organic Matter From Drinking Water. *Ozone: Sci. Eng.* **1994**, *16*, 367–383. [[CrossRef](#)]
52. Brisset, J.-L.; Pawlat, J. Chemical Effects of Air Plasma Species on Aqueous Solutes in Direct and Delayed Exposure Modes: Discharge, Post-Discharge and Plasma Activated Water. *Plasma Chem. Plasma Process.* **2016**, *36*, 355–381. [[CrossRef](#)]
53. Kanazawa, S.; Kawano, H.; Watanabe, S.; Furuki, T.; Akamine, S.; Ichiki, R.; Ohkubo, T.; Kocik, M.; Mizeraczyk, J. Observation of OH Radicals Produced by Pulsed Discharges on the Surface of a Liquid. *Plasma Sources Sci. Technol.* **2011**, *20*, 034010. [[CrossRef](#)]
54. Buxton, G.V.; Greenstock, C.L.; Helman, W.P.; Ross, A.B. Critical Review of Rate Constants for Reactions of Hydrated Electrons, Hydrogen Atoms and Hydroxyl Radicals ($\cdot\text{OH}/\cdot\text{O}-$ in Aqueous Solution. *J. Phys. Chem. Ref. Data* **1988**, *17*, 513–886. [[CrossRef](#)]
55. Lide, D.R. *CRC Handbook of Chemistry and Physics*, 87th ed.; CRC Press: Boca Raton, FL, USA, 2006.
56. Siegrist, R.L.; Crimi, M.; Simpkin, T.J. (Eds.) *In Situ Chemical Oxidation for Groundwater Remediation*; SERDP/ESTCP Environmental Remediation Technology; Springer New York: New York, NY, USA, 2011; Volume 3, ISBN 978-1-4419-7825-7.
57. Abdelmalek, F.; Gharbi, S.; Benstaali, B.; Addou, A.; Brisset, J.L. Plasmachemical Degradation of Azo Dyes by Humid Air Plasma: Yellow Supranol 4 GL, Scarlet Red Nylosan F3 GL and Industrial Waste. *Water Res.* **2004**, *38*, 2339–2347. [[CrossRef](#)] [[PubMed](#)]
58. Depenyou, F.; Doubla, A.; Laminsi, S.; Moussa, D.; Brisset, J.L.; Le Breton, J.-M. Corrosion Resistance of AISI 1018 Carbon Steel in NaCl Solution by Plasma-Chemical Formation of a Barrier Layer. *Corros. Sci.* **2008**, *50*, 1422–1432. [[CrossRef](#)]
59. Njoyim-Tamungang, E.; Laminsi, S.; Ghogomu, P.; Njopwouo, D.; Brisset, J.-L. Pollution Control of Surface Waters by Coupling Gliding Discharge Treatment with Incorporated Oyster Shell Powder. *Chem. Eng. J.* **2011**, *173*, 303–308. [[CrossRef](#)]
60. Benstaali, B.; Addou, A.; Brisset, J.L. Electrochemical and X-Ray Investigation of Austenitic 304L and 316L Stainless Steels Treated by a Gliding Arc in Humid Air. *Mater. Chem. Phys.* **2003**, *78*, 214–221. [[CrossRef](#)]
61. Chang, J.-S. The Role of H₂O and NH₃ on the Formation of NH₄NO₃ Aerosol Particles and De-NO_x under the Corona Discharge Treatment of Combustion Flue Gases. *J. Aerosol Sci.* **1989**, *20*, 1087–1090. [[CrossRef](#)]
62. Mätzing, H. Chemical Kinetics of Flue Gas Cleaning by Irradiation with Electrons. *Adv. Chem. Phys.* **1991**, *80*, 315–402.
63. Peyrous, R.; Pignolet, P.; Held, B. Kinetic Simulation of Gaseous Species Created by an Electrical Discharge in Dry or Humid Oxygen. *J. Phys. D Appl. Phys.* **1989**, *22*, 1658. [[CrossRef](#)]
64. Tsagou-Sobze, E.B.; Moussa, D.; Doubla, A.; Hnatiuc, E.; Brisset, J.-L. Gliding Discharge-Induced Oxidation of a Toxic Alkaloid. *J. Hazard. Mater.* **2008**, *152*, 446–449. [[CrossRef](#)]
65. Janda, M.; Hensel, K.; Tóth, P.; Hassan, M.E.; Machala, Z. The Role of HNO₂ in the Generation of Plasma-Activated Water by Air Transient Spark Discharge. *Appl. Sci.* **2021**, *11*, 7053. [[CrossRef](#)]
66. Doubla, A.; Bouba Bello, L.; Fotso, M.; Brisset, J.-L. Plasmachemical Decolourisation of Bromothymol Blue by Gliding Electric Discharge at Atmospheric Pressure. *Dye. Pigment.* **2008**, *77*, 118–124. [[CrossRef](#)]

67. Pawlat, J.; Terebun, P.; Kwiatkowski, M.; Tarabová, B.; Kovaľová, Z.; Kučerová, K.; Machala, Z.; Janda, M.; Hensel, K. Evaluation of Oxidative Species in Gaseous and Liquid Phase Generated by Mini-Gliding Arc Discharge. *Plasma Chem. Plasma Process* **2019**, *39*, 627–642. [[CrossRef](#)]
68. Kim, J.Y.; Ballato, J.; Kim, S.-O. Intense and Energetic Atmospheric Pressure Plasma Jet Arrays. *Plasma Process. Polym.* **2012**, *9*, 253–260. [[CrossRef](#)]
69. Wan, M.; Liu, F.; Fang, Z.; Zhang, B.; Wan, H. Influence of Gas Flow and Applied Voltage on Interaction of Jets in a Cross-Field Helium Plasma Jet Array. *Phys. Plasmas* **2017**, *24*, 093514. [[CrossRef](#)]
70. Qaisrani, M.H.; Xian, Y.; Li, C.; Pei, X.; Ghasemi, M.; Lu, X. Study on Dynamics of the Influence Exerted by Plasma on Gas Flow Field in Non-Thermal Atmospheric Pressure Plasma Jet. *Phys. Plasmas* **2016**, *23*, 063523. [[CrossRef](#)]
71. Li, Q.; Li, J.-T.; Zhu, W.-C.; Zhu, X.-M.; Pu, Y.-K. Effects of Gas Flow Rate on the Length of Atmospheric Pressure Nonequilibrium Plasma Jets. *Appl. Phys. Lett.* **2009**, *95*, 141502. [[CrossRef](#)]
72. Borghi, C.A.; Cristofolini, A.; Grandi, G.; Neretti, G.; Seri, P. A Plasma Aerodynamic Actuator Supplied by a Multilevel Generator Operating with Different Voltage Waveforms. *Plasma Sources Sci. Technol.* **2015**, *24*, 045018. [[CrossRef](#)]
73. Shao, T.; Zhou, Y.; Zhang, C.; Yang, W.; Niu, Z.; Ren, C. Surface Modification of Polymethyl-Methacrylate Using Atmospheric Pressure Argon Plasma Jets to Improve Surface Flashover Performance in Vacuum. *IEEE Trans. Dielectr. Electr. Insul.* **2015**, *22*, 1747–1754. [[CrossRef](#)]
74. Wang, C. Effect of N₂ Jet on Si Electrode Surface in Dielectric Barrier Discharge. *IOP Conf. Ser.: Earth Environ. Sci.* **2020**, *440*, 022059. [[CrossRef](#)]
75. Trunec, D.; Navrátil, Z.; Tomeková, J.; Mazánková, V.; Ďurčányová, S.; Zahoranová, A. Chemical Composition of Gaseous Products Generated by Coplanar Barrier Discharge in Air and N₂/O₂ Mixtures. *Plasma Sources Sci. Technol.* **2022**, *31*, 115011. [[CrossRef](#)]
76. Burlica, R.; Locke, B.R. Pulsed Plasma Gliding-Arc Discharges With Water Spray. *IEEE Trans. Ind. Appl.* **2008**, *44*, 482–489. [[CrossRef](#)]
77. Royintarat, T.; Seesuriyachan, P.; Boonyawan, D.; Choi, E.H.; Wattanutchariya, W. Mechanism and Optimization of Non-Thermal Plasma-Activated Water for Bacterial Inactivation by Underwater Plasma Jet and Delivery of Reactive Species Underwater by Cylindrical DBD Plasma. *Curr. Appl. Phys.* **2019**, *19*, 1006–1014. [[CrossRef](#)]
78. Baier, M.; Janßen, T.; Wieler, L.H.; Ehlbeck, J.; Knorr, D.; Schlüter, O. Inactivation of Shiga Toxin-Producing Escherichia Coli O104:H4 Using Cold Atmospheric Pressure Plasma. *J. Biosci. Bioeng.* **2015**, *120*, 275–279. [[CrossRef](#)] [[PubMed](#)]
79. Dezest, M.; Bulteau, A.-L.; Quinton, D.; Chavatte, L.; Behec, M.L.; Cambus, J.P.; Arbault, S.; Nègre-Salvayre, A.; Clément, F.; Cousty, S. Oxidative Modification and Electrochemical Inactivation of Escherichia Coli upon Cold Atmospheric Pressure Plasma Exposure. *PLoS ONE* **2017**, *12*, e0173618. [[CrossRef](#)]

Disclaimer/Publisher's Note: The statements, opinions and data contained in all publications are solely those of the individual author(s) and contributor(s) and not of MDPI and/or the editor(s). MDPI and/or the editor(s) disclaim responsibility for any injury to people or property resulting from any ideas, methods, instructions or products referred to in the content.